BOUNDARY-LAYER MODELLING OF NEUTRAL AND STABLY-STRATIFIED FLOW OVER HILLS, WITH EMPHASIS ON THE DRAG

Peter A Taylor[1], Wanmin Gong[2], Yoseph Mengesha[1], Wensong Weng[1], Dapeng Xu[1] and Jingnan Zhou[1]
[1]York University, [2]Atmospheric Environment Service
Toronto, Canada

Summary: At the present time models of neutrally-stratified boundary-layer flow over hills, with Reynolds-averaged flow equations and various turbulence closure schemes, can, in general, do quite well at predicting the "speed-up" of the wind at the summit of isolated low and moderate slope hills, and on the upwind slope. Predictions in the lee of hills with flow separation are more difficult but some progress has been made. It is however proving extremely difficult to obtain reliable results for the form or pressure drag on topography in neutrally stratified flows. For stably stratified flow linear inviscid theory provides a first estimate of the wave drag. In a boundary-layer context some initial model results on pressure and wave drag are discussed. Difficulties in terrain representation are briefly discussed and some initial results of an analysis of the "sandhills" area are described.

1. INTRODUCTION

Although there have been some large eddy simulations of turbulent boundary-layer flow over topography (see for example results reported in *Gong et al*, 1996) most model studies to date have involved solutions of the ensemble-averaged flow equations with various forms of turbulence closure. *Ayotte et al* (1994) provide solutions with a range of alternative closures for simple 2D flows. Some models have been based on analytic solutions following various approximations to the governing equations (e.g. *Jackson and Hunt*, 1975; *Mason and Sykes*, 1979; *Hunt et al*, 1988a,b), some on the numerical solution to equations that have been linearised in terms of the topographic slope (*Beljaars et al*, 1987; *Ayotte et al*, 1994), and some solve the non-linear equations by either finite differences (e.g. *Wood and Mason*, 1993; *Ying and Canuto*, 1997) or an iterative, spectral method (*Xu and Taylor*, 1992; *Xu et al*, 1994). Many of the papers have focused on solutions for the flow over idealised, often 2D, terrain, although many of the models are applicable, at least in principle, to real 3D terrain. This is especially true of the linearised models and *Walmsley et al* (1982), *Taylor et al* (1983) and *Beljaars et al* (1987) provide illustrations of such applications.

Some tests of models against wind tunnel and field experimental observations have been conducted. There is generally good agreement between model results and observations of terrain induced variations in the mean wind speed on the upwind side of hills and at the summit, even in situations where linear models are used somewhat beyond their expected range, as noted by *Beljaars et al* (1987) and *Walmsley and Taylor* (1996). Models are generally less successful in predicting the variation of the turbulence statistics, especially above the "inner layer" - to be defined below, but higher order closure schemes (see *Ayotte et al*, 1994; *Ayotte*, 1993) do appear to give predictions that are qualitatively correct and in accord with rapid distortion theory. For instance even though the mean velocity, U, increases significantly above a hilltop, the standard

deviation, σ_u, decreases except very close to the surface (see for example *Mickle et al*, 1988). *Ying and Canuto* (1997) have recently made some comparisons between predictions from their 2D model with second order closure and the wind tunnel experiments of flow over hills reported by *Khurshudyan et al* (1981). There is generally good agreement for vertical profiles of mean velocity and σ_u (at the three locations for which results are presented), qualitative agreement in uw profiles but σ_w profiles are less satisfactory, especially in the lee of the hill. No pressure drag results are reported.

One significant exception to the generally satisfactory agreement between models and observations of mean wind speed is reported in *Taylor et al* (1997) where results from the NLMSFD (non-linear mixed spectral finite difference) model of *Xu et al* (1994) - XAT hereafter - are compared with observations made by *Gong et al* (1996) in a wind tunnel study of the airflow over a train of periodic two dimensional sinusoidal waves of the general form,

$$z_s(x) = a \text{ Cos } kx. \tag{1}$$

The wavenumber, $k = 2\pi/\lambda$ where λ is the wavelength of the waves. The maximum slope of the waves was $ak = 0.5$. Two surface roughnesses were used. In the relatively rough case with $\lambda/z_0 = 1.5 \times 10^3$ the flow separated in the troughs but there was still reasonable agreement between observed and predicted mean velocity profiles (Figure 1a). In the relatively, though not aerodynamically, smooth case, $\lambda/z_0 = 2.0 \times 10^4$ and the flow remains essentially attached. There is however a serious discrepancy between the observed and predicted mean velocity profiles, especially above the wave crests (Figure 1b). This may be linked to the observation that the flow over the 2D waves develops a 3D secondary flow in the form of longitudinal vortices aligned with the flow. *Phillips et al* (1996) argue that this is a form of Craik-Leibovich instability which should also be present over random rolling terrain. *Miller* (1995), who confirmed Gong et al's results in a separate wind tunnel study, found however that these features were not present in several examples of more complex two dimensional topography. In our ongoing numerical modelling of the development of these vortices (in collaboration with Stefano Gallino) we find that they only occur for waves of sufficient steepness (typically $ak > 0.3$) and that their growth rate, which has a non-linear dependence on slope, is substantially less than we observed in the wind tunnel experiments. In an unpublished extension of the work reported in *Gong et al* (1996), we also obtained wind tunnel results for the flow over a single smooth wave ($\lambda/z_0 = 2.0 \times 10^4$, $ak = 0.5$)) with,

$$z_s(x) = a(1 + \text{Cos } kx) \quad \text{for } -\pi < x < \pi \tag{2}$$

and zero elsewhere. In this case model predictions of velocity profiles (Figure 1c) and surface pressures

were again satisfactory, allowing that the model has a different background flow (constant stress layer with a logarithmic velocity profile) to that observed in the wind tunnel, where the boundary layer depth was approximately equal to the wavelength of the waves (λ).

We have introduced this case as a warning that, although in what follows we will use periodic sinusoidal waves as canonical examples of topography, there may be situations where this terrain has special complications of its own. At present our assessment is that stable longitudinal vortices will only develop in special cases, perhaps including the airflow over water waves, and that for typical terrestrial topography, either single hills or general rolling or mountainous terrain, they are unlikely to occur.

2. SOME PRELIMINARY CONSIDERATIONS

2.1 Typical Scales

In general the hills that are being considered in the models to be discussed are relatively small scale, not too steep and relatively smooth, both in terms of topography and ground cover. We implicitly assume a spectral gap between the resolved topography and the roughness elements, although in practice this may be hard to identify.

Jackson and Hunt (1975 - JH hereafter) divided the flow over low hills into inner and outer layers. In the outer layer, perturbations to the shear stress associated with the flow over the hill are assumed to be of no dynamical significance and the flow can be treated as essentially inviscid. The inner layer, of depth l_i, is defined by the height at which the perturbation stress gradient ($\partial uw/\partial z$), induced by flow over the hill, is of the same magnitude as the non-linear advection term ($U\partial U/\partial x$). The two terms combined will in turn approximately balance the pressure gradient ($\rho^{-1}\partial p/\partial x$). The estimate for l_i requires the assumption of a relationship between shear stress (τ) and velocity shear. Different assumptions lead to either (JH)

$$(l_i/L)\ln(l_i/z_0) = 2\kappa^2 \tag{3a}$$

or, *Jensen et al* (1984),

$$(l_i/L)[\ln(l_i/z_0)]^2 = 2\kappa^2 \tag{3b}$$

where L is defined as the upwind distance from the hilltop to the point where the elevation is half of the maximum. The Jensen et al formula leads to lower values for inner layer depth. Other formulae have been proposed, but all show that for hills with L of order 500m, the inner layer depth is of order 10m. An implication of the shallowness of the inner layer, exploited in the JH model, is that models with simple

turbulence closures, such as mixing length or E-*l*, schemes can give reasonable predictions of mean velocity and pressure perturbations even though their shear stress predictions in the outer layer are hopelessly wrong. One exception to this is in the precise phase of the surface pressure perturbation relative to the topography. This is critical for calculations of the pressure or form drag of the topography on the airflow, required for studies on the parameterization of the effects of sub-grid scale topography. The original JH model, which assumes inviscid irrotational flow in the outer layer and uses this as a basis for the pressure calculation, is unable to predict this drag.

For neutrally-stratified flow models the ideal application might be to an isolated hill with a characteristic length scale, L = 500m, height, h = 100m and surface roughness, z_0 = 0.01 - 0.1 m. Askervein (see *Walmsley and Taylor*, 1996) and several other hills on which field measurements have been conducted (*Taylor et al*, 1987), are quite close to this. The length limitation allows us to represent the approach or undisturbed flow as a constant stress or surface boundary layer with a simple logarithmic velocity profile for neutral stratification cases. This is not essential (see for example *Hunt et al*, 1988a) but has been used extensively to avoid introducing additional parameters associated with deeper planetary boundary layers. Note however that the topography will cause flow perturbations to heights of order L and the constant stress assumption will not really apply. Early comparisons between surface layer and PBL models by *Taylor* (1977) did however suggest that the surface-layer model is capable of accurate predictions of the near-surface flow.

There are many situations, especially in strong winds, where the boundary layer is well mixed in terms of potential temperature to heights of order 1km and the assumption of neutral stratification is valid. For longer hills, with L of order 10km or more, the presence of an inversion or stable layers aloft will generally require that these factors are considered. *Carruthers and Choularton* (1982) included these effects in their adaptation of the Jackson-Hunt model. The extension of numerical boundary-layer models of flow over topography to include stably stratified cases has been rather slow but some progress has been made and will be discussed below.

Assuming that we are dealing with winds of order $10ms^{-1}$ the time taken for air to flow over a hill of total length 4L = 2km will be only a few minutes and it is appropriate to seek steady state, time-independent solutions, except for some cases with steeper topography when there is a possibility of eddy shedding and non-steady wake flows. In the case of much longer wavelength topography (4L = 100km), where the advective time scale becomes several hours, a steady state is less appropriate. However it is still the simplest case to consider and avoids the introduction of numerous other parameters. The steady-state issue is also linked to the specification of the upstream, incident, background or undisturbed flow over flat terrain that

we consider to be perturbed by the presence of the topographic feature. The basic steady-state flow over horizontally homogeneous terrain can be either a constant flux "surface" layer or an equilibrium planetary boundary layer. If other background flows are specified then we need to consider their evolution (in time and space) in the absence of topography and either account for that in some way or suppress it. This is especially troublesome in the case of stably-stratified flows where constant flux layer formulations for the upstream flow inevitably lead to the trapping of topographically generated gravity waves since U increases steadily with height. The stably-stratified planetary boundary layer is continuously evolving in time or space and generally has a finite depth, above which the flow is essentially non-turbulent. These factors cause modelling complications.

3. LINEAR AND NON-LINEAR MODELS

In general we will not include detailed equations in this discussion paper since they are available elsewhere in the journal papers cited. We do however need to discus the basis for linear models and show how the results from linear models can be used to compute the non-linear pressure drag on topography.

The MSFD (mixed spectral finite difference) and NLMSFD (non-linear MSFD) models are based on the idea that the topography produces a perturbation to a steady, non-evolving flow over horizontally homogeneous flat terrain. In a neutral surface-layer context this will be either a constant shear stress layer with constant pressure, constant TKE and a logarithmic velocity profile or, in a planetary boundary-layer (PBL) context, these will be barotropic "Ekman spiral" solutions appropriate to the closure assumed, and in general obtained numerically as the steady state solution to the equations for flow over a horizontally homogeneous surface (see *Ayotte and Taylor*, 1995) . We denote these background flow variables with a subscript 0, as $\Phi_0(Z)$, where $\Phi(x,y,Z)$ could be a horizontal or vertical velocity component, U, V, W, pressure, P, turbulent kinetic energy, E, or a Reynolds stress component, uw, uu etc. Here Z represents height above the terrain ($z-z_s$), but in stratified flow cases it is sometimes convenient to use $\Phi_0(z)$ for potential temperature and pressure fields. The topography is then assumed to introduce perturbations $\alpha\Phi_1(x,y,Z)$ where $\Phi = \Phi_0 + \alpha\Phi_1$. The "flag" α is introduced here to indicate the perturbation terms and can be used to identify terms of zero, first and higher orders. In the case of 2D sinusoidal terrain (Equation 1) we will set $\alpha = ak$. Substituting these expressions into the governing equations provides a set of equations for the perturbation variables. For instance the steady state form of the U component surface layer (no rotation) momentum equation becomes,

$$U_{k0}\partial U_{i0}/\partial x_k + \alpha U_{k1}\partial U_{i0}/\partial x_k + \alpha U_{k0}\partial U_{i1}/\partial x_k + \alpha^2 U_{k1}\partial U_{i1}/\partial x_k$$

$$= -(1/\rho)\partial P_0/\partial x_i - \alpha(1/\rho)\partial P_1/\partial x_i - \partial \langle u_i u_k \rangle_0/\partial x_k - \alpha\partial \langle u_i u_k \rangle_1/\partial x_k \qquad (4)$$

The zero order terms (no α) should satisfy the equation anyway and so cancel out (as discussed earlier). In the linear MSFD model the higher order terms (in this case just α^2) are neglected and so Equation (4) and others like it give a set of linear partial differential equations, which we can write symbolically as,

$$L(\underline{\Phi}_1, f_1) = 0 \tag{5}$$

where $\underline{\Phi}_1$ represents the perturbation variables and the topography has the form $z_s = \alpha f_1(x,y)$. The operator L can depend on the zero order terms and Z but should have no x or y dependence. We solve these by first applying Fourier transforms in the horizontal directions (x and y) and then solving the sets of simultaneous ordinary differential equations in Z as boundary value problems for each of the horizontal wavenumber pairs (k,l). Details of the method, and a discussion of the weaknesses of the initial value "shooting" method used by *Beljaars et al* (1987) are given in *Karpik* (1988). This is a direct method for solving for the Fourier transformed variables and will generally yield a solution.

In the NLMSFD model we collect together all of the non-linear terms in Equation (4) - and similar equations, and place them on the right hand side of Equations (5), i.e.

$$L(\underline{\Phi}_1, f_1) = R(\underline{\Phi}_0, \underline{\Phi}_1, f_1) \tag{6}$$

The right hand side is non-linear in $\underline{\Phi}_1$ and is not suitable for Fourier transformation as it stands. We attempt to solve Equations (14) iteratively via

$$L(\underline{\Phi}_1^n, f_1) = R(\underline{\Phi}_0, \underline{\Phi}_1^o, f_1) \tag{7}$$

where $\underline{\Phi}_1^n$ and $\underline{\Phi}_1^o$ are the "new" and "old" estimates of the solution for $\underline{\Phi}_1$. Fourier transforms of R have to be evaluated at each iteration. For low slope terrain this non-linear correction works well and typically converges rapidly (in O(10) iterations). This makes it a highly efficient solution technique. As the topography steepens, increasing α, convergence is slower and eventually fails.

Once one goes beyond simple closure schemes the complexity of the equations, coupled to the splitting of the variables into background and perturbation components, leads to extremely complex equations, sometimes containing O(100) terms. To cope with this *Ayotte* (1993) and XAT wrote MAPLE procedures to both do the necessary algebra and then produce Fortran or C++ code for the computations.

XAT, *Xu and Taylor* (1995) and *Li* (1995) discuss the accuracy of the linear solutions in comparison with

the non-linear results. In general noticeable differences in velocity perturbation predictions start to appear for ak $>$ 0.1 and are significant for ak $>$ 0.3. For the calculated form drag however, despite non-linear variations in the amplitude, shape and phase of the perturbation surface pressures, non-linear effects appear to be small (XAT, *Xu and Taylor*, 1995). Figure 2 from XAT illustrates the variation in the surface maximum value of fractional speed-up ratio ($\Delta S = u_1/U_0$) and normalised form drag with wave slope. Note first that the linear, MSFD model predictions of fractional speed-up ratio have a linear variation with ak. The same will be true of the pressure perturbation, so that the form drag, a wavelength integrated product of surface pressure and slope, as predicted by the linear model, is quadratic in (ak). These calculations were performed with a 2nd order LRR turbulence closure (*Launder et al*, 1975) with and without (BLA) the inclusion of horizontal diffusion terms. Note that the linear and non-linear solutions match much better when the upper boundary condition, imposed at $Z = \lambda$, is on velocity rather than stress.

4. FORM DRAG ON SMALL SCALE TOPOGRAPHY

Although the consistency between linear and non-linear model predictions of drag, shown in Figure 2, may be dependent on turbulence closure, upper boundary conditions and terrain shape, it does offer some hope that results from linear models can be used to determine topographic drag in practical applications to real terrain, where slopes are often $<$ 0.3. Since the linear model surface pressure result for complex topography is a summation of results for individual Fourier components we should be able, in principle, to establish a "look-up" table of surface pressure results for individual (2D) wavenumber vectors and a range of λ/z_0 values and combine these with the spectrum of the terrain to determine the normalised neutral form drag coefficient for any grid square, subject to the model assumptions (periodic terrain, moderate slope, uniform roughness). These calculations would be based on the basic expression for form drag, i.e,

$$\int\int p\left(\frac{\partial z_s}{\partial x}, \frac{\partial z_s}{\partial y}\right) dx dy \qquad (8)$$

For simple terrain (e.g. Equations 1 or 2) inviscid, non-stratified flow theory would predict (dynamic) pressure minima above hilltops, maxima in valleys and zero form drag. The effect of the boundary-layer shear and turbulence is to slightly shift these pressure extrema downwind relative to the terrain, so that the integral above is no longer zero. The phase shifts are however generally small and the form drag calculation depends critically upon their precise value. This tends to be strongly dependent on the turbulence closure assumed within the model, although the amplitude of the pressure perturbations are relatively insensitive to closure. Typical drag differences are illustrated by Figure 3, also from XAT, showing a factor of about 3 between the form drag predictions of simple E-κz closure (high drag) and LRR and q^2l second order closure (low drag) models. Note also the effect of different surface roughness on these predictions of form drag.

We should comment that *Mason* (1991), at an ECMWF workshop, proposed a somewhat simpler formulation for form drag on low slope terrain. In terms of drag per unit area, which we denote as F_P, this gives,

$$F_P = C\rho u_{*0}^2\Theta^2 \tag{9}$$

where C is, in general, a function of λ/z_0 (λ is wave length and z_0 is roughness length), ρ is air density and u_{*0} is the friction velocity in the absence of topography. θ denotes the maximum slope of the undulation and equals ak in simple 2D sinusoidal terrain. For steep terrain they propose a fairly conventional drag coefficient, proportional to frontal area, in the form,

$$F_P = 0.5C_d\rho U_A^2 A_f/A_s \tag{10}$$

where C_d, a non-dimensional drag coefficient, is chosen to be 0.4. A_f is the frontal silhouette area, A_s is the horizontal area for which the drag is being computed and U_A is a velocity scale, for which Mason suggests that we take $\overline{U}(h/2)$, where the overbar indicates an areally averaged value and h is the height of the topography. For our sinusoidal waves $A_f/A_s = ak/\pi$ and, in Equation (10), F_P is proportional to slope rather than slope squared. *Wood and Mason* (1993) propose a universal form for all slopes of terrain.

It is perhaps worth emphasising that the drag produced by relatively low slope hills in neutrally stratified flows may be quite modest, especially if we believe the predictions of the relatively high order closure models. If we take Mason's formula (Equation 9) we see that the form drag is less than the skin friction (ρu_{*0}^2) for 2D terrain slopes, $\theta < C^{-1/2}$. With XATs recommendations for typical values of A (5 for 2D ridges and 2 for 3D terrain) the slopes at which form drag = skin friction with the "low slope" formula are 0.45 for 2D sinusoidal ridges and 0.71 for 3D sinusoidal terrain of the form z_s = a Cos kx Cos ky. At these slopes the flow may well separate and in any case the linear model predictions are suspect. For slopes more typical of many hilly areas of the globe (0.1 - 0.3) our present expectation is that the overall drag increases due to the presence of topography will be relatively modest (< 50%) in comparison with flow over flat terrain of the same surface roughness. Neutrally stratified flows with significant flow separation and stably stratified flows with gravity waves initiated by the topography may however produce much larger drag enhancement.

Returning to the wind tunnel experiments of *Gong et al* (1996) we can add that the initial motivation of that study was as a simple experiment to measure the surface pressure distribution and compute the form drag over 2D sinusoidal terrain for comparison with our model predictions. Maximum terrain slope was 0.5 in this experiment. Table I shows that the computed form drag (F_p) was significantly larger than the skin

friction ($<\tau_{fric}>$) in this experiment, both for the relatively smooth (with attached flow) and relatively rough (causing separated flow) surfaced waves. The wind tunnel drag values, when normalised by free stream velocity squared, were in general agreement with other (water tunnel) measurements over smooth surfaced waves, see *Gong et al* (1996, Figure 6c). For slopes in the range $0.3 < ak < 0.8$ there is some scatter in these results but they are generally consistent with $F_P = 0.013(ak)\rho U_0^2$, and significantly higher than our NLMSFD model predictions. The drag is consistent with Mason's Equation (10) above in that there is a linear dependence on slope but equivalence of the numerical coefficients would require $U_A/U_0 \approx 0.45$. The large eddy simulations for this flow, reported by Gong et al and also given in Table I, predicted form drags that failed to match the observational data, although the surface pressure distributions appeared similar (Figure 4). The discussion above can perhaps serve to remind us that, especially in these neutral flow cases, the measurement and prediction of the form drag on topography is a difficult and delicate task. More measurement, both in the field and in the wind tunnel, would be a worthwhile endeavour.

5. STABLY STRATIFIED FLOWS.

Stably stratified flow over topography has a variety of possible patterns, which have been extensively investigated in the inviscid, non-turbulent case (see for example *Baines*, 1995). Much less has so far been published on stably stratified boundary-layer flows, although these flows have been considered by, for example, *Hunt et al* (1988b), *Coppin et al* (1994) and *Belcher and Wood* (1996). In some recent modelling studies of stably stratified surface and planetary boundary-layer flows over topography *Weng et al* (1997) and *Zhou et al* (1998a,b) have concentrated on linearized, 2D models of flow over ideal, periodic sinusoidal terrain (Equation 1). In their models the turbulent boundary layer is of limited vertical extent and above this the flow is assumed to have uniform velocity, U, and buoyancy frequency, N. For flow over 2D sinusoidal terrain of wavenumber k, as in Equation 1, the outer flow Froude number based on the length scale of the terrain, $F_L = Uk/N$, is a critical parameter, just as it is in the inviscid flow case. For $F_L > 1$ the internal waves caused by the flow over the terrain are evanescent and decay with height just as they do in the neutral case ($F_L = \infty$). However for $F_L < 1$ the terrain produces propagating gravity waves which can carry momentum and produce a wave drag. The negative surface (perturbation) pressure distribution in the $F_L < 1$ case has phase shifts of approximately $\pi/2$ (exactly so in inviscid flow) relative to the terrain with minimum pressure on the lee slope and maximum upstream of the crest. This phase shift leads to much higher pressure drag values than in the $F_L > 1$ case. The effect of the turbulent boundary layer reduces the drag to somewhat lower values, but the linear inviscid result for wave or pressure drag per unit horizontal area, expressed as,

$$F_p = \tfrac{1}{2}(F_L^{-2}-1)^{\frac{1}{2}}\rho U^2(ak)^2 \qquad (11)$$

provides a reasonable first estimate of the drag. With $F_L = 0.5$ and $U = 20u_*$, Equation (11) would give a pressure drag equal to skin friction when $ak = 0.054$, a far lower slope than we estimated for the equivalent neutral boundary-layer induced drag (0.45). If $ak = 0.5$ then $F_p = 87\rho u_*^2$.

In *Zhou et al*'s (1998a,b) linear model computations for the planetary boundary layer the effect of the boundary-layer on the surface pressure drag and the wave drag at upper levels is illustrated in Figure 5. In this plot WFLX is an estimate of $<UW>$ on horizontal surfaces while LDRG (which they call local drag) is the pressure drag across a streamline. Values are normalised by the inviscid result given above. For the $F_L = 0.628$ case we see that the surface pressure drag is reduced by about 12% relative to inviscid theory while the wave flux is reduced by about 19%. The difference corresponds to an additional drag on the boundary layer. We should caution that these results are for a relatively simple, low order turbulence closure and from a linear model. Further boundary-layer modelling of departures from inviscid theory are desirable, together with laboratory and field experiments.

The relatively small predicted departures from linear inviscid theory is supportive of present practice in sub-grid scale gravity wave drag parametrization in climate and weather forecast models, but note that the theory here is applied for outer flow values of U and N. The "Launching height" (at which U and N are determined) utilised in many parametrizations should, we believe, be determined by the topographic length scale. Many present schemes (e.g. *Lott and Miller*, 1997) use a fraction of the topographic height (rather than the length scale) for this purpose.

6. CHARACTERIZATION OF TOPOGRAPHY

Even if we had a perfect model of neutral and stratified boundary-layer flow over topography we would still have the problem of how to represent the topography of the whole of the land surface of the globe. An underlying assumption in our approach has been that there is a spectral gap between the "topography" and the "roughness elements". Although this is probably valid for grass and heather covered rolling hills, it may be less so for geologically younger mountains and terrain with steep slopes and sharp peaks or ridges. In practice we are also seriously constrained by the topographic data that are available, especially if global coverage is required.

In a preliminary investigation of topographic parameters appropriate for drag parametrization we have made a study of the Sand Hills area of Nebraska (USA). Digital topographic data of the Sand Hills terrain were obtained (free of charge) from USGS 1:250,000 DEMs via the world wide web (http://sun1.cr.usgs.gov/eros-home.html). The 1:250,000 DEMs cover a one degree by one degree block representing one-half of a standard 1 degree by 2 degree 1:250K scale map. [Data for Canada are available

through Geomatics Canada at a cost of $270 per file, to indicate one of the problems of undertaking global analyses!] Each DEM consists of a regular array of elevations referenced horizontally on the geographic coordinate (latitude, longitude) system of the World Geodetic System 1972 (WGS 72) or for few DEMs, the WGS 84. Elevations are in metres relative to mean sea level. Spacing of the elevations along and between each profile is 3 arc-seconds with 1201 elevations per profile. Three arc-seconds correspond to approximately 90 metres in the north-south direction and variable spacing in the east-west due to convergence of meridians as latitude increases (approximately 90 metres at the equator and approximately 60 metres at 50 degree latitude). The whole Sand Hills region comprises about six DEMs. This area was selected for analysis since we plan to analyze data collected in Aug 1980 by the NCAR Queen Air during low level flights over parts of the region. The area overflown has an extensive area of relatively regularly spaced, elongated ridges, of typical peak to trough height of order 75m and crest to crest separation of order 2km. Typical flight levels were about 100m above the terrain but no surface level data were available. We have however computed flight level drag coefficients $(u_*^2{}_{FLT}/(U^2+V^2)_{FLT}$ for different sections of the flight and compared these with the slope of the underlying terrain (at this stage the root mean square slope from the aircraft determined terrain heights along the flight path). At this stage all stabilities are included. These preliminary data indicate a potential for a significant increase in aircraft level drag coefficient with topographic slope. Horizontal turbulence values (σ_u) were about 20-40% higher than one might expect over flat terrain. Further analyses are in hand.

Using a Fortran code provided by Zephyr North (Burlington, Ontario, Canada) and a Geographic Information Systems (GIS), ARC/INFO, the DEM data format was converted to a lattice or grid of elevation points. However, the lattice constructed from this USGS 1 deg by 1 deg DEM are not immediately suitable for extracting the topographic parameters mentioned above, such as the analysis of slope, because the horizontal dimensions i.e., x and y coordinates, the ground units, are measured in latitude and longitude (arc seconds), whereas the z values, the elevation points, are measured in metres. The x, y, and z coordinates should have the same units of measurements to simplify calculations of slope, aspect ratio, etc., and the DEM was projected onto UTM (Universal Transverse Mercator) coordinates (zone 14) with false easting and northing. Three non-overlapping sub-regions were selected for analysis. Sample results for sub-region A1, where a qualitative assessment suggests that the terrain is uniformly rugged, are given in Table II for a range of grid resolution, details will be discussed below. A contour map is shown in Figure 6.

The parameters suggested by *Baines* (1995) to characterizing topography [z = h(x,y)] are the slope correlation, M, defined as the mean of the product of the slopes in x and y; the K value, defined by the sum of the mean square slopes in x and y divided by 2; and the L value, defined by the difference of the mean square slopes in x and y divided by 2. These are given by:

$$K = (<(\partial h/\partial x)^2> + <(\partial h/\partial y)^2>)/2 : L = (<(\partial h/\partial x)^2> - <(\partial h/\partial y)^2>)/2 :$$
$$M = <(\partial h/\partial x)(\partial h/\partial y)> \quad (12)$$

Here $<\ldots>$ represents a spatial average over the domain under consideration. The principal axis of the topography is the axis where the slope correlation vanishes and it is oriented at an angle θ to the x-axis, where θ is given by $\theta = \frac{1}{2}\arctan(M/L)$. This gives the direction where topographic variation as measured by the mean squared gradient is largest, and the direction for minimum variation is perpendicular to this. If the x and y coordinates are rotated to the principal axis with new x' and y' coordinates then the new values of K, L, and M relative to these axes and denoted by K', L', and M' are given by;

$$K' = K : L' = (L^2 + M^2)^{1/2} : M' = 0 \quad (13)$$

These values can also be used to calculate the aspect ratio γ, which describes the anisotropy of the terrain. γ is defined as:

$$\gamma^2 = <(\partial h/\partial y')^2>/<(\partial h/\partial x')^2> \quad (14)$$

In the domain considered, the Sand Hills terrain shows anisotropy with $\gamma = 0.723$; the principal angle θ is found to be about 102°. This is in agreement with the contour map, Figure 6, which shows that undulations are oriented in an approximately east-west direction. Table II lists the topographic parameters defined above for different grid resolutions. Many of the statistical topographic parameters are dependent on grid resolution and for K, L and M there is no indication of convergence as the resolution is increased. As the grid resolution increases, the slopes, especially the maximum slope, increase. Similar results were obtained by Jenson (1993) in her analysis of slope of the Chemung River (Finger Lakes, NY, USA) area. Some parameters such as the average and standard deviation of elevation converge rapidly as grid resolution increases. Others such as the principal angle θ appear to converge more slowly (to a value of 103° at the finest grid resolution of 100m). The drag however will be primarily dependent on slope and this presents an obvious problem to resolve.

7. ACKNOWLEDGEMENTS

Our research on boundary layer flow over topography is conducted with financial support from the Natural Sciences and Engineering Research Council of Canada and the Atmospheric Environment Service of Canada. Specific work on topographic drag is supported under a collaborative research agreement with the Canadian Climate Research Network.

REFERENCES

Ayotte, K.W., 1993: Higher order closure in turbulent flow over hills. PhD thesis, CRESS, York University, North York, Ontario, Canada.

Ayotte, K.W., Xu, D. and Taylor, P.A., 1994: The Impact of Different Turbulent Closures on Predictions of the Mixed Spectral Finite Difference Model for Flow over Topography, Boundary-Layer Meteorol., 68, 1-33.

Ayotte, K.W. and Taylor, P.A., 1995: A Simple, Linear, Three-Dimensional Model of Planetary Boundary-Layer Flow over Topography. J. Atmos. Sci., 52, 3523-3537.

Baines, P.G., 1995: Topographic Effects in Stratified Flows, Cambridge University Press, 482pp

Belcher, S.E. and Wood, N., 1996: Form and wave drag due to stably stratified flow over low ridges. Quart. J. R. Meteorol. Soc., 112, 863--902.

Beljaars, A.C.M., Walmsley, J.L. and Taylor, P.A., 1987: A mixed spectral, finite difference model for neutrally stratified boundary-layer flow over roughness changes and topography, Boundary-Layer Meteorol. 38, 273-303.

Carruthers, D.J. and Choularton, T.W., 1982: Airflow over hills of moderate slope. Quart. J. R. Meteorol. Soc, 108, 603-624.

Coppin, P.A., Bradley, E.F. and Finnigan, J.J., 1994: Measurements of flow over an elongated ridge and its thermal stability dependence: the mean field. Boundary-Layer Meteorol., 69, 173-199.

Gong, W., Taylor, P.A. and Dornbrack, A., 1996: Turbulent boundary-layer flow over fixed, aerodynamically rough, 2D sinusoidal waves. J. Fluid Mech., 312, 1-37.

Hunt, J. C. R., Leibovich, S. and Richards, K. J., 1988a: Turbulent shear flows over low hills. Quart. J. R. Meteorol. Soc., 114, 1435-1470.

Hunt, J. C. R., Richards, K. J. and Brighton, P.W.M., 1988b: Stably stratified flow over low hills. Quart. J. R. Meteorol. Soc., 114, 859-886.

Jackson, P.S. and Hunt, J.C.R., 1975: Turbulent wind flow over a low hill. Quart. J. Royal Meteorol. Soc., 101, 929-955.

Jensen, N.O., Petersen, E.L. and Troen, I., 1984: Extrapolation of Mean Wind Statistics with Special Regard to Wind Energy Applications. Rep. WCP-86, WMO, Geneva, 85 pp.

Jenson, S.K., 1993: Applications of hydrologic information automatically extracted from digital elevation models, in Terrain analysis and distributed modelling in hydrology, John Wiley & Sons, 35-47.

Karpik, S.R., 1988: An Improved Method for Integrating the Mixed Spectral Finite Difference (MSFD) Model Equations. Boundary-Layer Meteorol., 43, 273-286.

Khurshudyan, L.H., Snyder, W.H. and Nekrasov, I.V., 1981: Flow and dispersion of pollutant over two-dimensional hills, EPA-600/4-81-067, US EPA, Research Triangle Park, North Carolina.

Launder, B. E., Reece, G. J. and Rodi, W., 1975: Progress in the development of a Reynolds-stress turbulence closure. J. Fluid Mech., 68, 537-566.

Li, P.Y., 1995: A numerical study on energy transfer between turbulent airflow and finite amplitude water waves, PhD thesis, CRESS, York University, 181pp.

Lott, F. and Miller, M, 1997: A new subgrid scale orographic drag parametrization: its formulation and testing, Quart J. Roy. Meteorol. Soc., 123, 101-127

Mason, P.J., 1991: Boundary-layer parameterization in heterogeneous terrain, ECMWF workshop proceedings, Fine scale modelling and the development of parameterization scheme, 275-288.

Mason, P.J. and Sykes, R.I., 1979: Flow Over an Isolated Hill of Moderate Slope. Quart. J. Roy. Meteorol. Soc., 105, 383-395.

Mickle, R.E., Cook, N.J., Hoff, A.M., Jensen, N.O., Salmon, J.R., Taylor, P.A., Tetzlaff, G. and Teunissen, H.W., 1988: The Askervein Hill Project: Vertical Profiles of Wind and Turbulence. Boundary-Layer Meteorol., 43, 143-169.

Miller, C., 1995: Turbulent boundary-layers above complex terrain. PhD thesis, Boundary-Layer Wind Tunnel Laboratory, University of Western Ontario, London, Ontario, Canada, 235pp.

Phillips, W.R.C., Wu, Z. and Lumley, J.L., 1996: On the formation of longitudinal vortices in a turbulent boundary layer over wavy terrain. J. Fluid Mech., 326, 321-341.

Taylor, P.A., 1977: Numerical studies of neutrally stratified planetary boundary-layer flow above gentle topography I. 2D cases. Boundary-Layer Meteorol., 12, 37-60.

Taylor, P.A., Walmsley, J.L. and Salmon, J.R., 1983: A simple model of neutrally stratified boundary-layer flow over real terrain incorporating wavenumber dependent scaling. Boundary-Layer Meteorol. 26, 169-189.

Taylor, P.A., Mason, P.J. and Bradley, E.F., 1987: Boundary-Layer flow over low hills - A review. Boundary-Layer Meteorology, 39, 107-132

Taylor, P.A., Xu, D., Gong, W. and Ayotte, K.W., 1997: Modelling turbulent boundary-layer flow over 2D sinusoidal waves, The Air-Sea Interface, ed. M.Donelan, W.H.Hui and W.J.Plant, University of Miami Press. 15-20.

Walmsley, J.L., Salmon, J.R. and Taylor, P.A., 1982: On the application of a model of boundary-layer flow over low hills to real terrain. Boundary-Layer Meteorol. 23, 17-46.

Walmsley, J.L. and Taylor, P.A., 1996: Boundary-Layer Flow over Topography: Impacts of the Askervein Study. Boundary-Layer Meteorol., 78, 291-320.

Weng, W., Chan, L., Taylor, P.A. and Xu, D., 1997: Modelling stably stratified boundary-layer flow over low hills, Quart. J. Royal Meteorol. Soc., 123, 1841-1866.

Wood, N. and Mason, P. J., 1993: The pressure force induced by neutral, turbulent flow over hills, Quart. J. R. Meteorol. Soc., 119, 1233-1267.

Xu, D. and Taylor, P. A., 1992: A non-linear extension of the Mixed Spectral Finite Difference model for neutrally stratified flow over topography, Boundary-Layer Meteorol., 59, 177-186.

Xu, D. and Taylor, P.A., 1995: Boundary-Layer Parameterization of Drag over Small Scale Topography. Quart. J. R. Meteorol. Soc., 121, 433-443.

Xu, D., Ayotte, K.W. and Taylor, P.A., 1994: Development of the NLMSFD model of turbulent boundary-layer flow over topography. Boundary-Layer Meteorol., 70, 341-367.

Ying, R. and Canuto, V.M., 1997, Numerical simulation of flow over two dimensional hills using a second order turbulence closure model, Boundary-Layer Meteorol. 85, in press.

Zhou, J, Taylor, P.A. and Qi, Y., 1997a, On stably stratified planetary boundary-layer flows over topography, subm to Boundary-Layer Meteorol. (Sept 1997).

Zhou, J, Taylor, P.A. and Qi, Y., 1997b, On wave drag, form drag and parameterization of sub-grid scale topography in large scale models, subm to Boundary-Layer Meteorol. (Oct 1997)

TABLE I

Drag values over sinusoidal waves - wind tunnel study

Surface Type	$(u_*^2)_0$	$<\tau_{fric}>$	F_p	$<\tau_{fric}>+F_p$	MTB
Relatively Smooth	0.0017	0.0025	0.0085	0.0110	0.0092
Relatively Rough	0.0038	0.0014	0.0065	0.0079	0.0127

All drag values are per unit area and are normalised by ρU_0^2, where U_0 is the freestream velocity. $(u_*^2)_0$ is the upstream or flat floor stress from the velocity profile; wavelength averaged $<\tau_{fric}>$ values are calculated assuming local logarithmic profiles near the surface with the roughness lengths determined from the upstream or flat floor measurements, F_p - normalised Form Drag, calculated from 2D equivalent of Equation 8, MTB - total drag computed from momentum budget over 10 waves.

Drag values over sinusoidal waves - LES results

Surface Type	$<\tau_{fric}>$	F_p	$<\tau_{fric}>+F_p$
Rel Smooth	0.0020	0.0027	0.0047
Rel Rough	0.0016	0.0054	0.0070

All drag values are per unit area and are normalised by ρU_0^2. They are based on LES results at $t = 16\ T_{ref}$, where T_{ref} = Wavelength/U_0. $<\tau_{fric}>$ is the horizontal force on the surface due to friction and F_p is the normalised Form Drag as above.

TABLE II

Topographic Parameters of the SANDHILLS region (A1) for various grid resolutions

Grid Resolution	17x17 1600m	33x33 800m	65x65 400m	129x129 200m	257x257 100m
Topographic parameter					
$<h>$	1135.5	1134.5	1133.9	1133.7	1133.7
σ_h	24.7	23.6	23.3	23.3	23.3
S(x)	0.0281	0.0494	0.0975	0.185	0.270
RMSS(x)	0.848E-02	0.149E-01	0.243E-01	0.320E-01	0.370E-01
S(y)	0.0237	0.0644	0.116	0.165	0.255
RMSS(y)	0.793E-02	0.148E-01	0.310E-01	0.431E-01	0.495E-01
K	0.675E-04	0.221E-03	0.773E-03	0.144E-02	0.191E-02
L	0.450E-05	0.749E-06	-0.185E-03	-0.418E-03	-0.541E-03
M	0.673E-05	-0.320E-04	-0.152E-03	-0.219E-03	-0.255E-03
θ	28.1	135.7	109.7	103.8	102.6
K'	0.675E-04	0.221E-03	0.773E-03	0.144E-02	0.191E-02
L'	0.809E-05	0.320E-04	0.239E-03	0.472E-03	0.598E-03
γ	0.886	0.864	0.727	0.712	0.723
RMSS(x')	0.869E-02	0.159E-01	0.318E-01	0.437E-01	0.501E-01

Notes: Topographic Notations

$<h>$ = Average height : σ_h = Standard deviation of height ;

S(x), S(y) = Maximum slopes in x, y-direction

RMSS(x), RMSS(y). RMSS(x') = Root mean square slope in x, y and x' directions

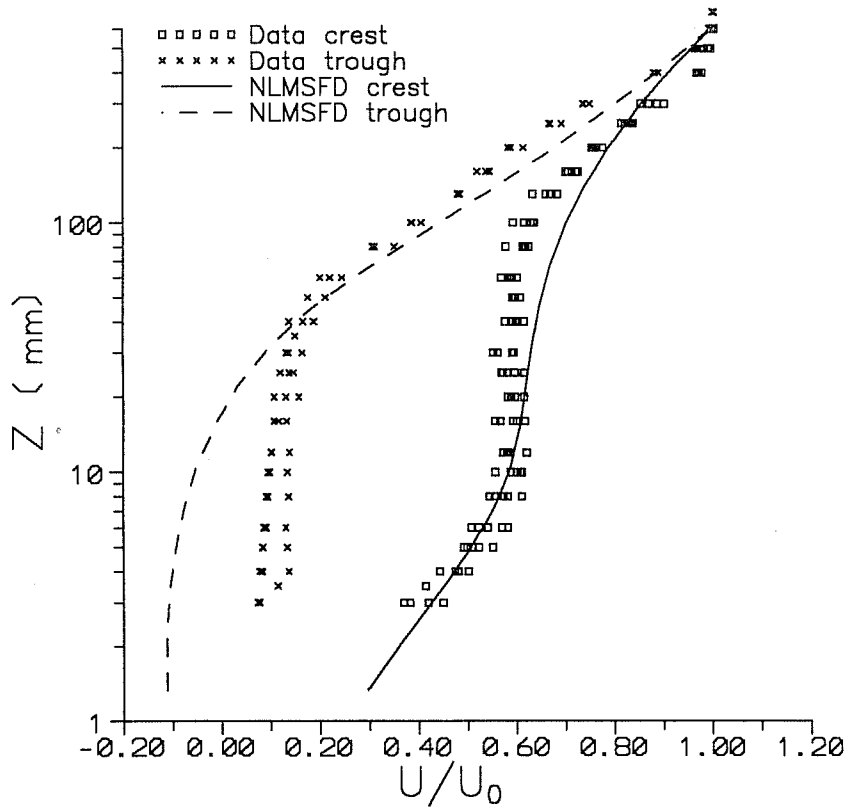

Figure 1 Mean velocity profiles above the crests and trough of a fixed sinusoidal wave with ak = 0.5. Wind tunnel data and NLMSFD results with E-κz closure.
a) From the 11th of 16 waves (x - trough, □ - crest) with $\lambda/z_0 = 1.5 \times 10^3$ (relatively rough), From Taylor et al (1996).

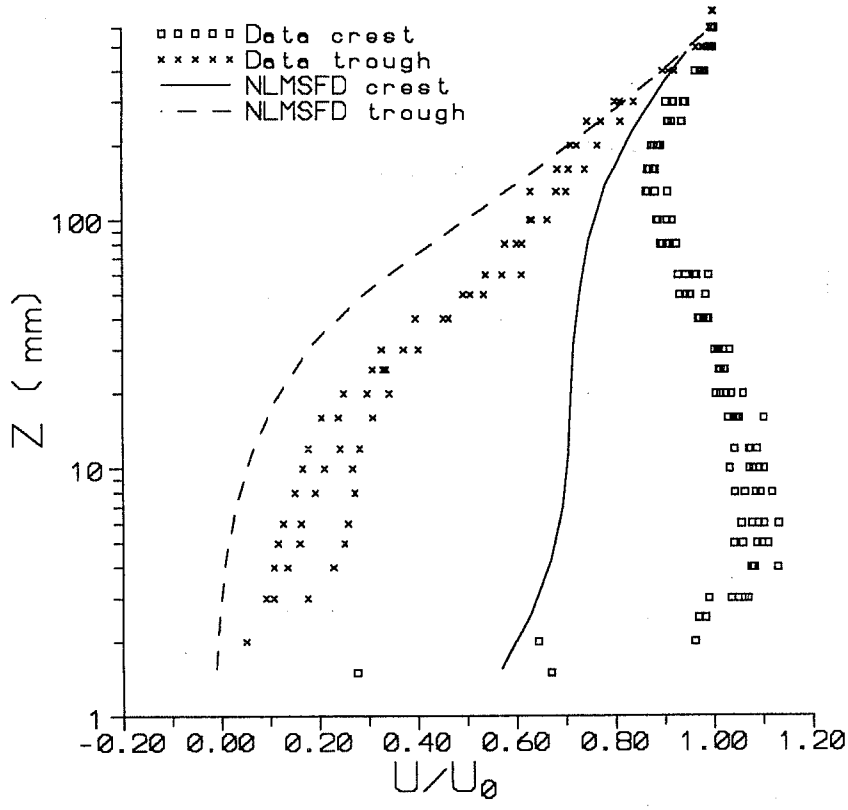

Figure 1 b) Same as (a) but $\lambda/z_0 = 2 \times 10^4$ (relatively smooth)

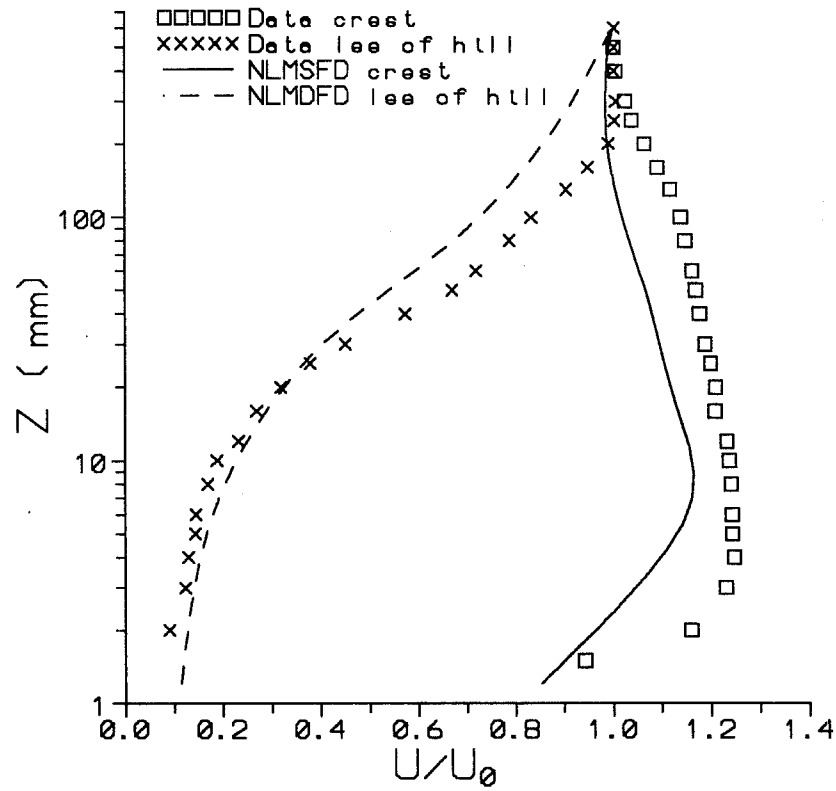

Figure 1 c) Velocity profiles above the crest and in the lee of an isolated hill, $\lambda/z_0 = 2x10^4$ (relatively smooth).

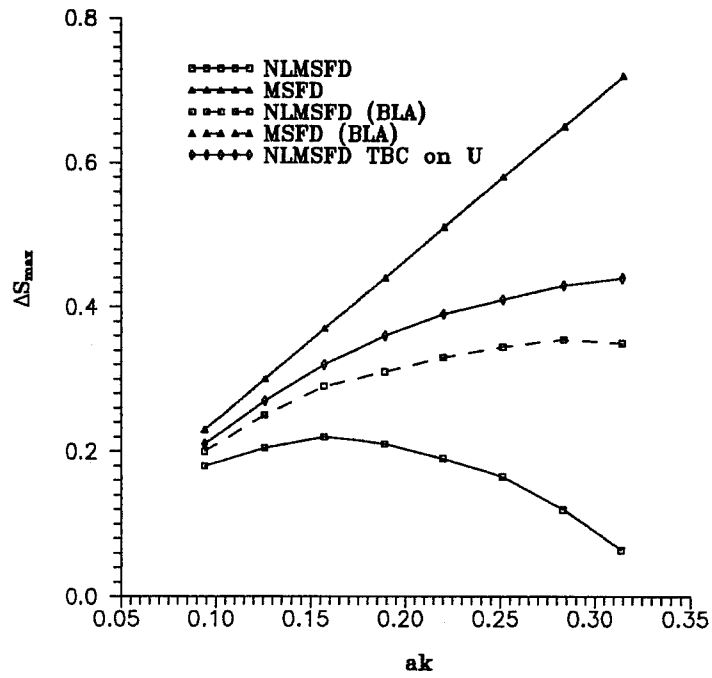

Figure 2a Maximum fractional speed-up ratio at the crest versus slope. LRR closure, 2D sinusoidal terrain, $\lambda/z_0 = 10^4$. From Xu et al (1994).

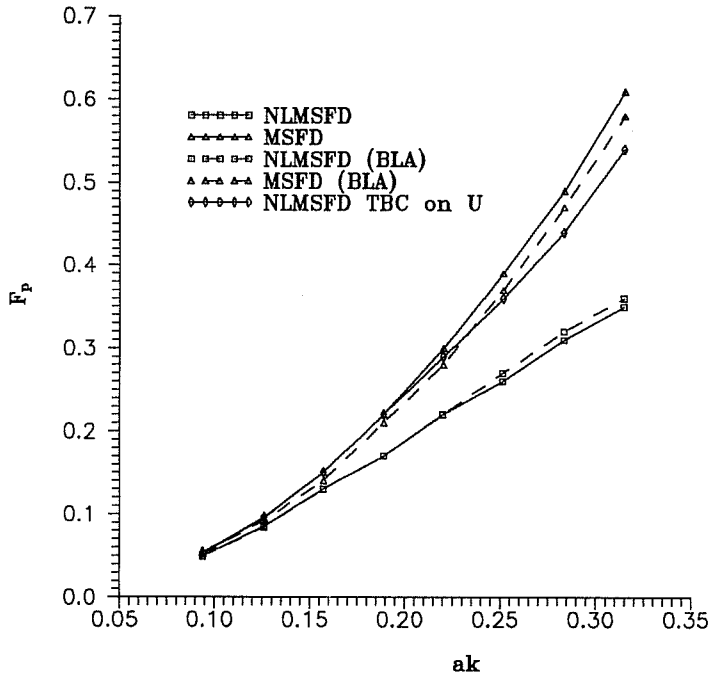

Figure 2b Form drag (b) versus slope. LRR closure, 2D sinusoidal terrain, $\lambda/z_0 = 10^4$. From Xu et al (1994).

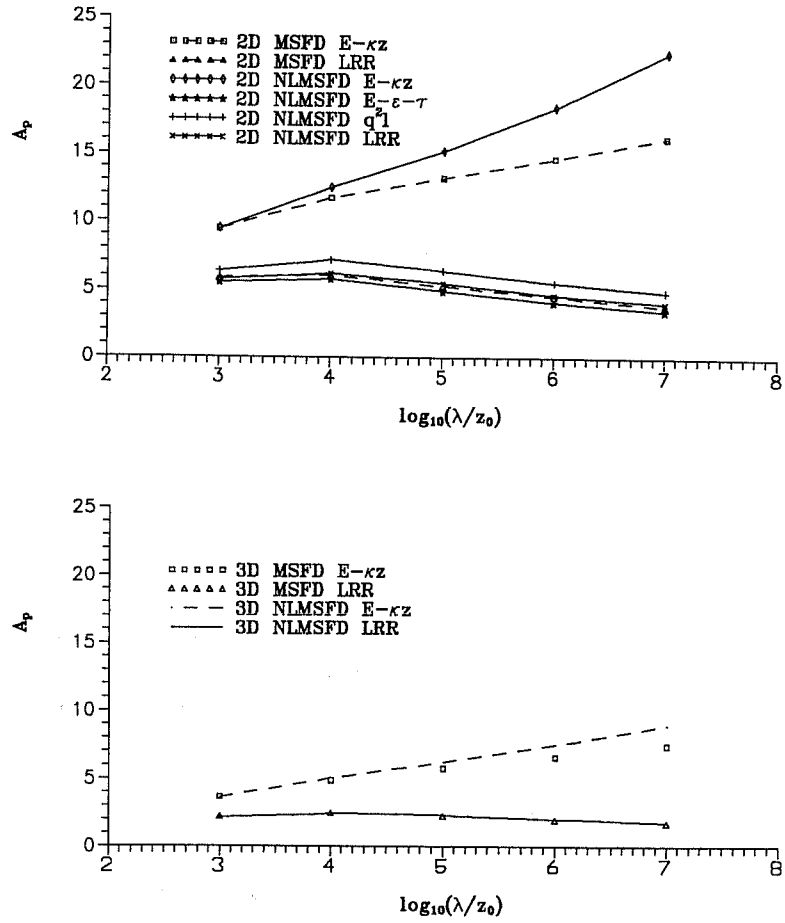

Figure 3 Form drag coefficient A_p, a) ak=0.157, 2D, b) ak=al=0.157, 3D. From Xu et al (1994).

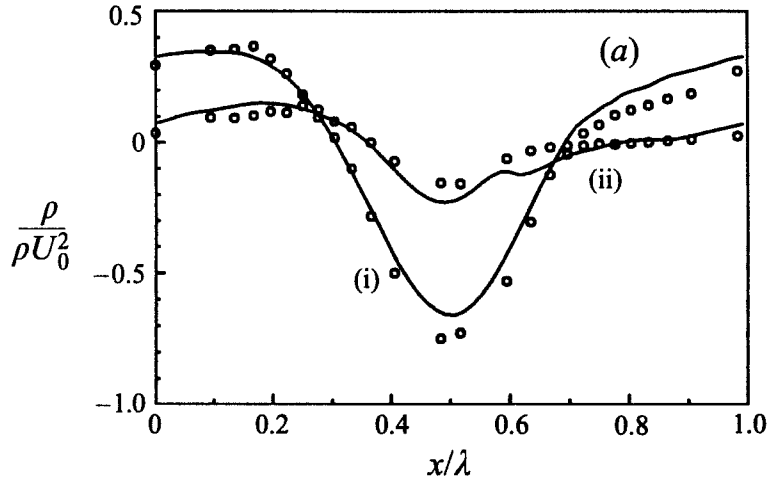

Figure 4 Surface pressure ($p/\rho U_0^2$) over sinusoidal waves (10th wave), (o) measurements, and LES predictions, curve (i) - relatively smooth surfaced waves (z_0 = 0.03mm); curve (ii) - relatively rough waves (z_0 = 0.4mm). From Gong et al (1996).

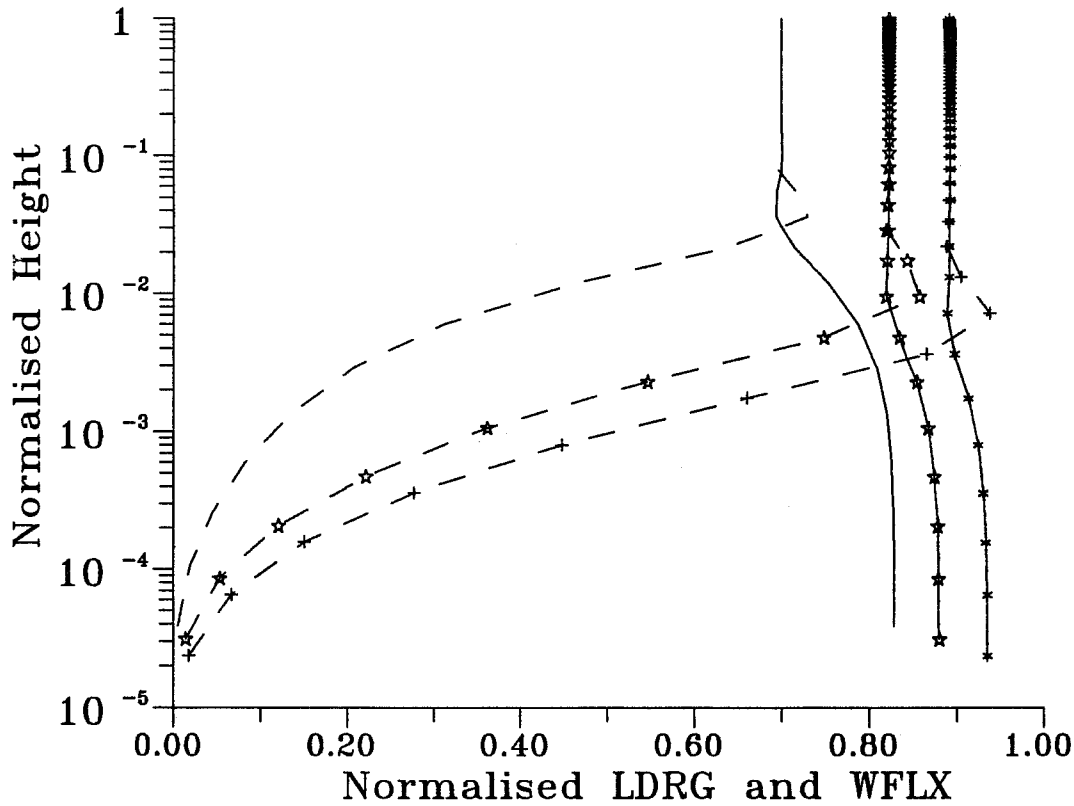

Figure 5 Profiles of the normalised forces on different surfaces in stably stratified planetary boundary layer flow over sinusoidal terrain. Streamline, δ=constant (LDRG - continuous lines); horizontal surface, z=constant (WFLX - dashed lines). z_0=0.1m, u_g=10m/s, and N=0.01s^{-1}. No symbol, Wavelength = 100km, F_L = 0.0628; * Wavelength = 10km, F_L = 0.628; + Wavelength = 7.5km, F_L = 0.837. Linear model results from Zhou et al (1998b). Height is normalised by $\lambda(F_L^{-2} - 1)^{-1/2}$.

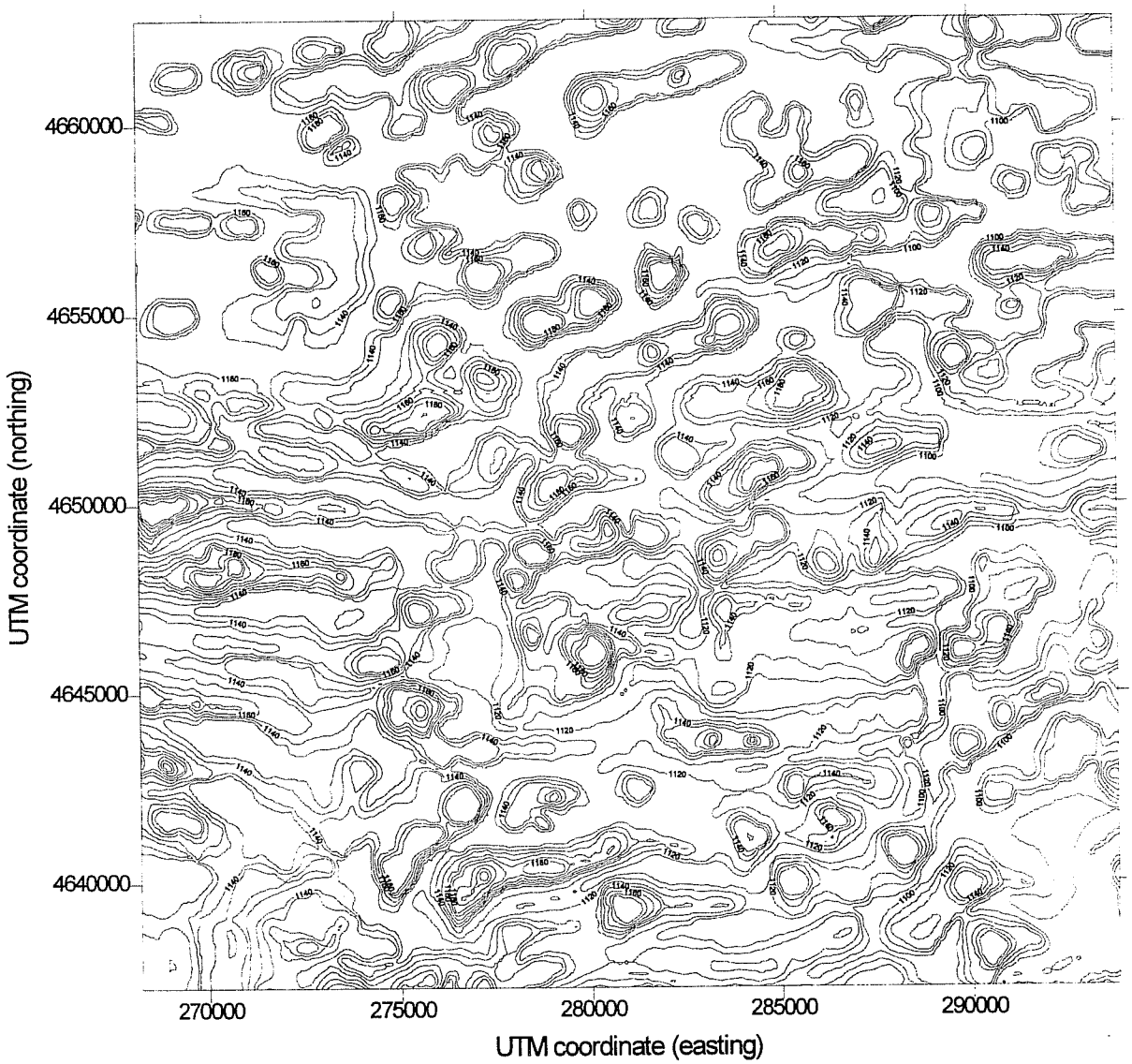

Figure 6 Contour map of a 25.6km x 25.6km portion (A1) of the Nebraska Sandhills region used for topographic analysis. Contour interval 10m.